Egypt. J. Chem. **Vol. 66** No. 11 pp. 685 – 700 (2023)

Egyptian Journal of Chemistry

http://ejchem.journals.ekb.eg/

Recent Advances in Sensors

Medhat Ibrahim[a] and Ahmed Refaat[a,b,*]

[a]*Molecular Spectroscopy and Modeling Unit, Spectroscopy Department, National Research Centre, 33 El-Bohouth Str. 12622 Dokki, Giza, Egypt*

[b]*Synchrotron-Light for Experimental Science and Applications in the Middle East (SESAME), Allan, JORDAN*

Abstract

Sensors are used in so many different aspects of our daily life. Extensive scientific research work has been carried out for years to develop and fabricate sensors for different applications, and using different materials and preparation methods. In addition, several different analytical techniques, including spectroscopic, electrical, optical, and chemical techniques are continuously employed to assess the performance of the fabricated sensors. The ongoing work aims to develop sensors for newly emerging applications, as well as improve the performance of the commonly used classes of sensing materials in terms of higher sensitivity and selectivity, faster response times, and better recovery and limits of detection. This review highlights the recent advances in sensor technology, covering different types of sensors applied in everyday life including biosensors, gas, humidity, temperature, and smoke sensors, as well as molecular modeling approaches in studying sensing mechanisms of different structures.

Keywords: Sensors; Biosensors; Gas; Humidity; Temperature; Modeling

1. Introduction

Sensors are devices that detect and quantify an input stimulus, either directly or by converting this stimulus to a signal for processing by other special systems. The output signals are essentially functionally related to the input stimuli which are generally referred to as measurands [1]. Sensors can quantify everything of physical, chemical, and/or biological concern, such as temperature, concentration, light intensity, and heart rate [2].

The development of sensors started as early as the second century (Fig. 1) and has been going on ever since. In recent years, there has been an increasing demand for the development of different sensor systems with a diversity of applications, which consequently requires tailored designs to provide novel approaches and solutions.

When designing a sensor, both technical and economic aspects of the desired application should be considered, aided by previous well-known sensor elements and structures, as well as simulation models to effectively shorten the fabrication time, and optimize the sensor properties and performance [3].

Different ways can be used to classify or categorize sensors. They can be classified based on their mode of operation into passive or active sensors, or based on input/output signal-conversion mechanism, into, for example, thermoelectric, electrochemical, photoelectric, thermo-optic, and electromagnetic sensors [4].

A wider method of classifying sensors is to classify them based on their applications such as temperature sensors, smoke sensors, gas sensors, humidity sensors, and biosensors [4].

*Corresponding author e-mail: ahmed.refaat@sesame.org.jo.

Receive Date: 01 June 2023, **Revise Date:** 11 July 2023, **Accept Date:** 31 July 2023

DOI: 10.21608/EJCHEM.2023.214821.8071

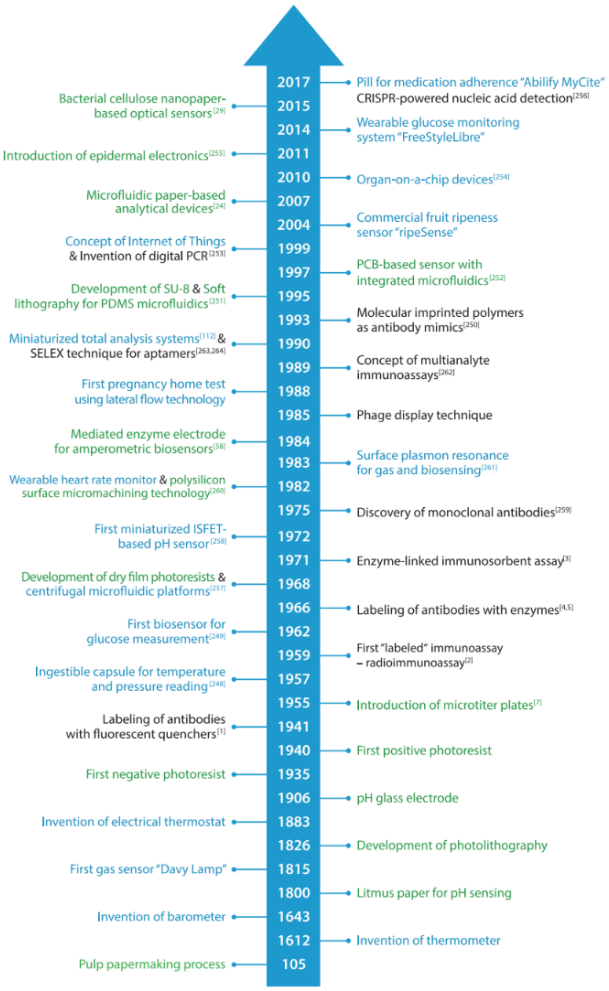

Fig. 1: Timeline of sensor development technology. This figure was reproduced with permission from Dincer et al.[2]

(https://creativecommons.org/licenses/by/4.0/)

2. Types of sensors based on their application

2.1. Gas sensors

The release of different gases requires continuous development in the design and fabrication of gas sensors, to improve the detection and quantification of these gases, and to control their levels [5]. Gas sensors are designed for and capable of detecting the presence of many dangerous gases, such as those of toxic or explosive nature, in addition to volatile organic compounds, and are also able to quantify them [6]. Gas sensors are commonly designed using metal oxides [6] and carbon nanomaterials [5], in addition to thin polymer films and electrochemical solid-state galvanic cells [7].

Using iron oxide (α-Fe_2O_3) nanorods with enhanced sensitivity and selectivity by zinc oxide (ZnO) nanoparticles were synthesized by Touba and Kimiagar [8] using a hydrothermal method. Their results confirmed that ZnO-decorated α-Fe_2O_3 significantly enhanced the sensing properties towards different alcohols and gases, in terms of faster sensor response and higher intensity sensing response, compared to pure α-Fe_2O_3 nanorods. This enhancement was attributed to the formation of more than one depletion zone on the surface of the nanocomposite, leading to decreased resistivity.

Zubair and Akhtar [9] synthesized sensors based on ZnO nanostructures with novel morphologies to detect ethanol, acetone, and ammonia (NH_3) gases. The sensing properties of the as-prepared (ZnO-AP) ZnO nanostructures were compared with those of calcined (ZnO-Cal) and commercial (ZnO-Com) nanostructures. At room temperature (29 °C), ZnO-AP and ZnO-Cal showed better performance towards 1 x 10^{-6} ammonia with gas responses of 63.79% and 66.87%, respectively. The corresponding response and recovery times recorded were 13 and 3 seconds, respectively. The better performance of ZnO-AP and ZnO-Cal nanostructures can be attributed to their unique morphology, as well as significant shape and size uniformity. On the other hand, the sensor based on ZnO-Com was not able to detect concentrations of NH_3 gas less than 200 x 10^{-6}, yet similar to ZnO-AP and ZnO-Cal was more selective towards ammonia than to ethanol and acetone and ethanol.

Kulkarni S.B. et al [10] also successfully synthesized an NH_3 gas sensor based on a nanocomposite of polyaniline and tungsten oxide (PANI-WO3) on polyethylene terephthalate (PET) substrate. At room temperature, the best performance obtained of the fabricated flexible sensor was that of the composition of 50 wt% WO_3, which demonstrated very high selectivity towards 100 ppm of NH_3 with the highest recorded response of 121% and a significantly stable response of 83%. Quantification and verification of the gas sensing behavior of flexible PANI-WO_3 sensors were also tested against ambient air and NO_2 gas. They concluded that these prepared cost-effective hybrid nanocomposites with their room temperature operation have numerous applications in the industrial market and domestic areas.

Diniz M.O. et al. [11] developed an NH_3 gas sensor with enhanced performance from a hybrid PANI derivative, poly(o-methoxy aniline) (POMA)-vanadium pentoxide (V_2O_5) film, and using a newly developed AC electrical measurement approach. Complex impedance results indicated high sensitivity of the layer-by-layer deposited POMA/V_2O_5 hybrid film to ammonia in both real and imaginary components, with linearity in response in the 0–20 ppm range, indicating that the film is a good candidate as a sensor for ammonia.

The molecular imprinting technique has been utilized by Abdelghani R. et al. [12] to develop nano-architectured SnO_2–based sensors with high

sensitivity for Acetone and NH_3 gases. SnO_2 films were synthesized using spin coating, with NH_4OH or acetone being introduced under different conditions during the hydrothermal synthesis. The performance of the fabricated sensors was tested against different substances, and results showed an increase in the response to the gases with increasing the participation of their respective solvents during the synthesis process. Results also demonstrated the high performance of the fabricated gas sensor devices reaching a sensitivity of about 90% for Ammonia gas and reaching the detection limit of 600 ppb when the sensor is patterned on NH_4OH and water, then rinsed by water. Regarding acetone, the sensor devices also demonstrated high sensitivity of about 77% and a detection limit of 280 ppb when the sensor is patterned on NH_4OH and acetone, then rinsed by acetone.

Chachuli S.A.M. et al. [13] developed a metal oxide/ multi-walled carbon nanotubes (MWCNT) gas sensor for hydrogen, based on TiO_2/MWCNT/B_2O_3 by comparing the sensitivity of this sensor with the addition of linseed oil and ethyl cellulose organic binders. Sensor composite was placed on an aluminum oxide substrate via the screen-printing method. To assess its performance, the proposed sensor was exposed to different concentrations of hydrogen ranging from 100 to 1000 ppm at 100 °C, 200 °C, and 300 °C operating temperatures. The addition of MWCNT in TiO_2 was found to reduce the bandgap and resistance, as well as reduce the optimal temperature of operation of the TiO_2 gas sensor, thus improving its sensitivity. The TiO_2/MWCNT/B_2O_3 gas sensor with different binders also demonstrated good responses to the different concentrations of hydrogen and at the different operating temperatures. In terms of response to hydrogen gas, the ethyl cellulose-based sensor was better than that based on linseed oil. Whereas in terms of conductive and recovery time, the linseed oil-based sensor yielded better results. The results of this study also indicated that the best performance of the proposed sensor is achieved when operating at the temperature of 200 °C. Correlating the obtained results together, the authors concluded that the linseed oil–based sensor is a better candidate, owing to its better performance as well as the cost-effective fabrication process.

An approach was developed by Myadam N.L. et al. [14] to fabricate xerogels as sensors for formaldehyde gas, based on Al/SnO_2 via propylene oxide assisted sol-gel process, using varying Al doping ratios (1–4 mol%). To further reinforce the gel network, the fabricated xerogels were subjected to aging for one day, followed by sintering and screen-printed thick film formation. Results demonstrated that Al/SnO_2 with Al doping level of 3 mol% showed excellent gas sensing ability with gas response (Ra/Rg) of 15 at the operating temperature of 300 °C towards around 100 ppm formaldehyde concentration, with quick response of around 7 seconds and recovery time of around 16 seconds. Results also indicated that the 3 mol% Al-doped SnO_2 sample maintained approximately 89% of its initial sensitivity, until after 2 months of shelf-life.

In an attempt to produce a room-temperature gas sensor with improved resistance to humidity resistance and long-term stability, Gao Z. et al. [15] introduced a gas sensor based on TiO_2 nanotubes decorated with Pd nanoparticles (Pd/TiO_2 NTs) with a hydrophobic polydimethylsiloxane (PDMS) layer by a simple thermal evaporation process. Response of pristine Pd/TiO_2 NTs sensor decreased with the increase in relative humidity (RH), reaching around 10% response value at 75% RH in comparison to its response at RH of 25%. Whereas under optimized conditions, the PDMS-coated Pd/TiO_2 NTs demonstrated excellent humidity resistance. It has also been indicated that the performance of the sensor is strongly affected by the thickness of the PDMS layer, such that insufficient thickness of this layer was not able to make the gas sensor resistive to humidity despite their super hydrophobic nature. PDMS layer also provided significant protection against photodegradation by TiO_2, in comparison to previously applied protective organic layers, thus qualifying it for a long functionality time. It was concluded that the simple method of applying PDMS coating to the proposed sensor provides an effective approach for designing several gas sensors based on semiconductor metal oxides capable of operating at room temperature with enhanced humidity resistance and long-term stability.

Kohli N. et al. [16] reported the effect of introducing carbon nanotubes (CNT) by hydrothermal method into indium oxide (In_2O_3) nanobars on the structure, morphology, and electronic properties of the resulting nanocomposites, and their acetone sensing properties. Characterization techniques indicated that the nanocomposites were successfully synthesized with their desired enhanced physical properties. The In_2O_3/CNT nanocomposite sensors demonstrated a superior performance which is attributed to the increased surface area of sensing, as well as the presence of defects and the formation of p-n heterojunctions. Results also demonstrated that at an optimum operable temperature of 300°C, the fabricated sensors are capable of detecting the minimum concentration of 10 ppm of acetone with a sensor response magnitude of around 4. The obtained results suggest that the proposed sensors show great potential for medical and pharmaceutical applications such as measuring glucose levels.

Santhosh N.M. et al. [17] developed a gas sensor for ethanol based on entangled MWCNTs on polyurethane (PUR) after Ar plasma treatment and He plasma treatment. Sensors resulting from plasma treatment demonstrate higher sensitivity to different concentrations of ethanol as compared to untreated ones. The untreated sensors demonstrated no change

in their responses with increasing ethanol concentration, while both Ar and He plasma-treated sensors displayed approximately 5 times and 3 times improvement, respectively, with increasing ethanol concentration. In comparison to the untreated sensors, results also demonstrated a stable sensitivity of the treated ones for the following ~14 days after their synthesis. Results also demonstrated that the treated sensors showed a faster response as well as a faster recovery. No significant morphological changes were associated with plasma treatment, suggesting that the improved performance of the treated sensors is most likely due to the enhanced surface properties induced by plasma treatment, and resulting in the development of sensitive functional groups to ethanol vapor, which was confirmed by the presence of additional peaks after plasma treatment in the resulting infrared spectra.

Using the radiofrequency (RF) magnetron sputtering method, Mustaffa S.N.A. et al. [18] successfully fabricated ZnO thin films optimized for sensing H_2 gas at 27°C. The prepared films were subjected to further optimization before testing their sensing performance. Results indicated that the RMS surface roughness of the annealed sample slightly decreased with a slight improvement in its optical properties, while the optimized films demonstrated a decreased energy gap. Results of the sensing experiment reported an increase in the calculated molar extinction coefficient with the increase of RMS surface roughness, suggesting that a relatively increased roughness increases the affinity of the films to optically absorb H_2 gas. It was concluded that the optical sensing properties of the RF-sputtered ZnO thin films to 2 mol% H_2 are highly dependent on the surface morphology of the sample, with the optical absorption of H_2 gas significantly increasing with higher surface roughness.

Using a simple precipitation method, Vinh N.T. et al. [19] synthesized a sensitive film of Fe_3O4/FeOOH nanocomposites deposited by the spray-coating method on a quartz crystal microbalance (QCM) for high-performance gas sensing applications. The sensing performance of the nanocomposite-based QCM sensor was evaluated at room temperature against different concentrations of CO, NO_2, and SO_2. The presence of numerous OH functional groups in the nanocomposites introduced plenty of interaction sites to the sensing layer of this mass-type gas sensor. The gas sensing results indicated that the developed sensor has good sensing performance toward toxic gases at room temperature. The developed nanocomposite-based QCM, therefore, offers a low-cost gas sensor with very good performance.

Strauss I. et al. [20] synthesized UiO-66 and UiO-66-NH_2 nanocrystals via a solvothermal method to be used in CO_2 gas sensing devices. Results confirmed that the functionalization of UiO-66 with –NH_2 groups significantly improved its sensitivity towards CO_2. FTIR results proved the affinity of the synthesized crystals towards as low CO_2 concentrations as 20 ppm. Results also indicated that the existence of water molecules enhanced the performance of UiO-66-NH_2 by increasing CO_2 adsorption compared to the absence of water. UiO-66-NH_2 was found to be significantly more sensitive to CO_2 than UiO-66. Based on FTIR and dielectric spectroscopy results, the authors concluded that UiO-66-NH_2 is suitable for application in sensing devices for both low and high CO_2 concentrations, while UiO-66 is relatively not suitable for capacitive CO_2 sensing.

An enhanced NO_2 gas sensor device was developed by Umar A. et al. [21] based on supramolecular assembled PANI/silver oxide/graphene oxide (PANI/Ag_2O/GO) composites. These composites were considered resistor-based sensors, highly responsive to NO_2 gas, and their sensing performance was examined at different temperatures. The highest sensitivity demonstrated by PANI/Ag_2O/GO sensor devices was 5.85 for 25 ppm of NO_2 at the optimized temperature of 100 °C, while pure PANI and PANI/Ag_2O composites showed less sensitivity.

An H_2S gas sensor was fabricated based on SnO_2–Fe_2O_3 nanocomposite, deposited on a printed substrate with interdigitated electrodes and tested in the air [22]. Impedance spectroscopy presented the semiconducting nature of the prepared nanocomposites with an activation energy of 0.13 ± 0.01 eV. Sensing results indicated that the fabricated sensors demonstrated excellent performance owing to their ability to operate at room temperature and for as low concentrations of H_2S as 2.5 ppm. The characteristics of the synthesized nanocomposites and their excellent sensing performance highly suggest their applicability as portable gas sensors.

Thangamani and Khadheer [23] using the solution-casting method prepared polyvinyl formal (PVF)/titanium dioxide (TiO_2) nanocomposite films and evaluated them as chemiresistive sensors for the detection of SO_2 gas in comparison to pristine TiO_2 nanoparticles. Results indicated that the pristine TiO_2 NPs showed a maximum sensitivity of 50.25% at 370 °C while PVF/TiO2 nanocomposite demonstrated a significantly improved sensitivity of 83.75% for the concentration of 600 ppm of SO_2 gas at a relatively low operating temperature of 150 °C, with also improved selectivity, faster response (66 seconds) and recovery (107 seconds), and extended stability of 60 days.

A facile cost-effective hydrothermal technique was also utilized by Thangamani and Khadheer Pasha [24] to synthesize copper (II) oxide nanoparticles (CuO-NPs) and tested as a chemiresistive sensor for detecting chemical vapors of benzene, toluene, ethylbenzene, and xylene (BTEX) with concentrations

ranging from 40 ppm up to 1000 ppm at 160 °C as an optimum operating temperature. The sensing results indicated that the CuO-NPs sensor is capable of detecting BTEX gas, as well as showing high sensitivity and fast response/recovery for toluene gas under different relative humidity conditions.

Sholehah A. et al. [25] successfully fabricated an ethylene gas sensor using a ZnO-Ag layer on a flexible polyethylene terephthalate-indium doped tin oxide (PET-ITO) substrate. Correlating their structural and morphological properties with their sensing performance, results showed that the best-achieved sensitivity to ethylene gas is with a smaller crystallite size ZnO-Ag layer. Results also demonstrated that the best performance was achieved by the sensor composed of the ZnO-Ag layer containing 0.6 mM of Ag, which showed a 5.65% response to 30 ppm concentration of ethylene gas for a 15-minute exposure time, and a 16.01% response to 100 ppm concentration. The recovery time recorded was 10 minutes and 15 minutes, respectively.

Light-activated chemoresistive sensors to detect NO_2 and acetone gases were also fabricated by Drozdowska K. et al. [26] based on nanoporous NiO films prepared by advanced gas deposition. Resulted confirmed that sensitivity towards NO_2 significantly increased under 275 nm UV irradiation. Improved sensitivity was also recorded at an elevated temperature of 150 ˚C. The obtained FTIR spectra depicted the formation of nitro and nitrate groups on the surface after exposure to NO_2 gas in synthetic air. UV light activation enhanced the sensing ability of NiO films owing to promoting interband transition in NiO which, in turn, induces the formation of electron-stimulated nitro and nitrate ions on the surface, thus explaining the improved performance of the sensor after UV activation. The sensing of acetone, on the other hand, causes a permanent breakdown of the reaction products which, consequently, accumulate on and cover the surface of the sensor, decreasing its sensitivity.

Kumar H. et al. [27] designed and developed a novel amperometric sensor using CuO quantum dots-decorated PANI plastic nanocomposites as a gas sensor for formaldehyde. Different electrochemical characterization techniques supported by theoretical computational calculations were utilized to assess the sensing performance, stability, and reusability of the prepared nanocomposite sensor for 720 hours. Faradaic and capacitive currents were measured at definite concentration, time, and potential, and the results demonstrated a linear current-concentration response with a correlation coefficient of 0.997. Characteristic electrochemical peaks were observed, confirming the presence of formaldehyde and, hence, the capability of the proposed nanocomposite sensor to detect formaldehyde. The developed sensor showed great potential as a fast and reliable sensor for quantitative and qualitative determination of environmental pollutants, that does not require immobilization of specific macromolecules for the sensing process.

A selective chemiresistive sensor for NH_3 and CO gases at room temperature based on PANI/GO nanocomposite was synthesized by Mohammed H.Y. et al. [28] using an in-*situ* chemical oxidation polymerization method. The sensor device is composed of pure PANI and PANI/GO nanocomposite cast on a low-cost pattern of Cu-interdigitated electrodes. Results indicated that the sensing behavior of PANI/GO nanocomposite-based sensors was preferable to NH_3 than to CO and that they showed superior performance for NH_3 than those of pure PANI. The PANI/GO-based sensor showed a high response of 9.6%–70 ppm, a fast recovery time of 23 seconds, and a low detection limit of 30 ppm, with a linear dynamic range of 30–230 ppm. It also showed outstanding sensing parameters for NH_3 such as stability, reproducibility, and repeatability.

Umar A. et al. [29] prepared and studied a supramolecularly assembled isonicotinamide–GO nanocomposite (Iso-rGO) and Iso-rGO/Carbon felt (CF) electrode (illustrated in Fig. 2) as NO_2 gas sensor at room temperature. Evaluation of the sensing performance of the fabricated sensor also demonstrated a superior reductive behavior of NO_2 gas at room temperature. The linear range of detection ranged from 1 up to 30 ppm, with a remarkably low limit of detection of 1 ppm concertation of NO_2 gas. Sensing results were also consolidated and confirmed by the results obtained from online gas chromatography. The performance of the sensor was also tested in the presence of other interfering gases, where it showed an acceptable selectivity towards NO_2 gas. The obtained results qualify the proposed electrode as a suitable sensor for NO_2 gas in real samples.

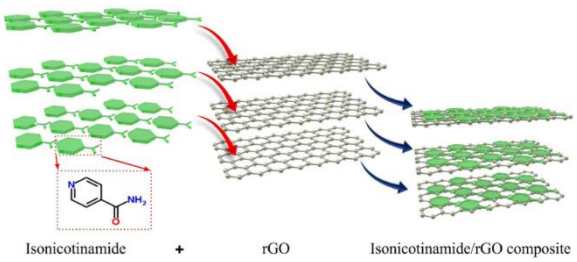

Fig. 2: Synthesis of isonicotinamide–graphene oxide nanocomposite. This figure was reproduced with permission from Umar et al.[29] (https://creativecommons.org/licenses/by/4.0/)

2.2. Temperature sensors

Temperature sensors are currently applied in various fields including industry, agriculture, and healthcare, in addition to their long-known common applications in the control of different devices such as air conditioning control and freezers [4].

Based on silver nanowires [AgNWs], Li S. et al. [30] introduced a facile method to fabricate AgNWs-based temperature sensors intended to detect variations in body temperature. Results demonstrated a quantifiable linear relationship between temperature and the resistance of AgNWs films. Results also indicated that by applying a protective layer of polydimethylsiloxane (PDMS) films to AgNWs random network to control the effect of humidity, the sensitivity of the fabricated sensor to temperature reached approximately 16 Ω/℃ over the range of 30–80 ℃. They concluded that the integrated PDMS-AgNWs temperature sensor which combines the low cost and excellent conductivity of AgNWs with the protective behavior PDMS against humidity, in addition to temperature sensitivity and good reproducibility, provide a promising strategy for further development of temperature sensors.

Relying on the temperature dependence of the electrical conductivity of conductive polymers, organic temperature sensors, Nitani M. et al. [31] constructed a poly(3,4-ethylenedioxythiophene) (PEDOT)-based conductive polymer as a temperature sensor. Using inkjet printing, the sensor was fabricated in the form of patterned resistors of PEDOT-based polymer. The patterned resistors demonstrated a −0.75%/°C temperature coefficient of resistance at 23 °C. The results obtained in this method were comparable to those obtained by metal resistors which were used as references. Results suggested that the fabricated sensors could operate at a long temperature range from -10 °C up to 80 °C under normal conditions.

Kumar V. et al. [32] presented epitaxial silicon carbide (SiC) as a circular-shaped Ni/4H-nSiC Schottky barrier diode (SBD) highly sensitive and linear temperature sensors. The fabricated sensors had an area of 3.140 mm^2 and their sensing performance was characterized in the forward current (I_f) range of 10 pA to 5 nA, and temperature range of 233 K–473 K. Results indicated that the highest absolute thermal sensitivity value reached was 3.425 mV/K at the minimum I_f of 10 pA. The best performance achieved by the fabricated sensors was at an I_f of 0.1 nA with the lowest temperature error of 1.620 K and the highest coefficient of determination of 99.96%. The maximum operating temperature point of the fabricated sensors for $I_f \leq 20$ pA was found to be 448 K.

In an attempt to fabricate a highly precise and accurate temperature model in the process of biofermentation, an ultrahigh sensitive fiber-optic sensor was proposed by Liu and Yuan [33] to measure temperature changes. The proposed sensor was developed by arc discharge technique as single-mode optical fiber (SMF) coupled with a urethane acrylate (UA)-coated off-axis spiral long-period fiber grating (OAS-LPFG). Because the refractive index (RI) of both UA and SMF cladding are close, and owing to its high thermo-optic coefficient, the resonant wavelength of the OAS-LPFG dip is, therefore, highly sensitive to temperature. Results indicated that the sensor's temperature sensitivity can reach ~-108.69 nm/◦C, over a temperature range of 25.0 ◦C to 25.5 ◦C, which is considered higher sensitivity than other all-fiber-based temperature sensors.

Qiu S. et al. [34] proposed a toluene and gold wire-filled helically twisted photonic crystal fibers (HT-PCFs) as highly sensitive temperature sensors and investigated the influence of the structural parameters on the performance of the proposed HT-PCF sensor. Results indicated that the optimized HT-PCF demonstrated a relatively high average sensitivity of 14.35 nm/℃ (from –20 ℃ to 20 ℃), and 17.29 nm/℃ (20 ℃ to 70 ℃). The proposed temperature sensor is also found insensitive to the hydrostatic pressure. It was concluded that this temperature sensor can be a very suitable candidate for different environmental and medical applications.

Liu S. et al. [35] proposed a temperature sensor with enhanced sensitivity using harmonic Vernier effect-based cascaded Sagnac loops. Results revealed a temperature sensitivity of about 3.66 nm/℃ in the range of 30–70 ℃, which is significantly higher than the sensitivity of a single Sagnac loop (0.163 nm/℃) by 22.5 times, and also higher than the sensitivity of the sensor based on basic Vernier effect (2.12 nm/℃) by 1.7 times. The authors concluded that the developed sensor can be widely applicable in certain fields, such as the mining industry and power grids.

Wang X. et al. [36] evaluated and analyzed the temporal drift characteristic, as an important performance parameter, of inkjet-printed silver nanoparticles-poly(3,4-ethylenedioxythiophene) polystyrene sulfonate (Ag NPs-PEDOT:PSS) flexible temperature sensor, shown in Fig. 3. Evaluation was performed through temperature range of 0–150 ºC. Results demonstrated an increase in the drift error by 0.91 kΩ at 0 ◦C, and 0.85 kΩ at 150 ◦C. The performance of the proposed sensor device can be studied in terms of three different variables related to the substrate, water molecules, and/or silver nanoparticles, which offers the opportunity to propose different solutions to any drawbacks in the sensor's performance.

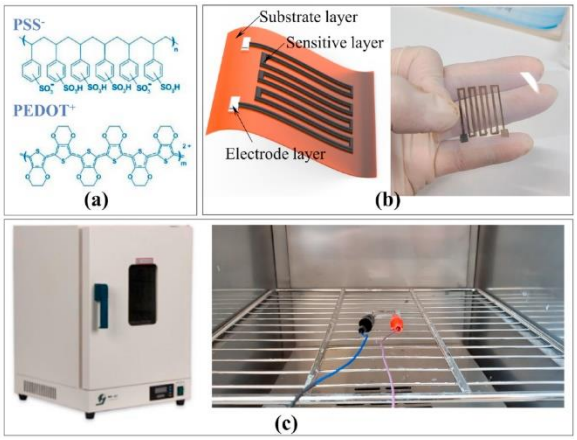

Fig. 3: (a) Molecular structure of PEDOT:PSS; (b) Fabricated flexible sensor. (c) Drift characterization of the fabricated sensor. This figure was reproduced with permission from Wang et al.[36] (https://creativecommons.org/licenses/by/4.0/)

Schepperle M. et al. [37] developed a platinum microheater/temperature sensor array for direct yet non-invasive heating and temperature measurement at several locations along microchannels. The working platinum area of each element in the array was as minute as 238 nm in thickness, 0.1 mm in width, and 0.5–2 mm in length. Results indicated that the fabricated microstructures can operate up to the maximum temperature of 450 ºC with a linear resistance coefficient to temperature of around 2.98 x 10^{-3} $ºC^{-1}$, and a relatively very low measurement error below 0.05%.

2.3. Humidity sensors

These sensors are used to detect and quantify water vapor, representing what is known as relative humidity (RH). They are widely applied for controlling heating, ventilation, and air conditioning systems, which in turn serve different applications which include preserving pharmaceuticals and controlling preservation conditions in museums, greenhouses, meteorological stations, and hospitals [4].

Kim H.-S. et al. [38] fabricated a low-resistance humidity sensor based on Core-shell-structured Chitosan-MWCNT (CS-MWCNT) on a gold electrode, where the resistance of the sensor device changes upon the formation of hydrogen bonds between water and NH_2 groups of CS. The CS-MWCNT nanohybrid humidity sensory containing 25% MWCNTs showed the highest response and linearity, independent from both voltage and frequency Results also indicated a fast (40 seconds) recovery time in the RH range of 30–100% and a long-term stability for 60 days, confirming the excellent performance of this humidity sensor.

Using bromothymol blue (BTB) as an indicator, titanium dioxide (BTB/TiO_2), palygorskite (BTB/palygorskite), and mullite (BTB/mullite) were chosen by Wang Z. et al. [39] as the host of colorimetric humidity sensor. A readable response by BTB/TiO_2 was observed to the RH of 11, 43, and 75% at 1 minute at 25 °C. BTB/palygorskite demonstrated a better response, especially at lower values of RH (~11%). Results indicated that the performance of the sensors was affected by the surface area and, hence, the cover density of BTB and water adsorption, which significantly enhanced their performances.

Capacitance-based TiO_2/Ag nanocomposite interdigital electrode was fabricated as a humidity sensor [40]. Resulted confirmed that the nanocomposite of TiO_2 nanoparticles containing a small amount of Ag nanoparticles greatly improved the sensitivity of the sensor. Results proved that the best mass ratio sample was TiO_2/Ag: 20:1 which showed the best sensitivity, reaching 10646.8 pf/RH%, which represents significantly higher performance than pure TiO_2. Results also demonstrated an increase in the sensor film's hydrophilicity, as well as the emergence of Warburg impedance at 11% RH in the complex impedance spectra plot, confirming the improvement that Ag provided to the absorption ability of the nanocomposite. It can be concluded that this proposed humidity sensor with its high sensitivity is capable of offering nondestructive detection of wet paper in the fields of preservation of ancient manuscripts and historical paintings.

An original humidity sensor based on a porous laser-induced-graphene electrode was developed by Zhu C. et al. [41] relying on its superior mechanical and electrical properties. The proposed sensor demonstrated outstanding performance over a wide range of RH (11–97%). Results also indicated the excellent performance of the sensor for breathing and fingertip non-contact motoring of this humidity sensor, qualifying it for applications in health sectors, especially in health monitoring devices.

Preparation and successful application of flexible polystyrene/polypyrrole (PS/PPy) mats as a resistive humidity sensor have been reported [42]. These composite membranes were obtained by incorporating PPy chains by an in situ chemical polymerization into electrospun PS films. Sensor performance results demonstrated that PS/PPy humidity sensors had a relatively high (128.6%) and fast (54.9 ± 3.5 seconds) sensing response, with a recovery time of 76.8 ± 11.1 seconds, with satisfactory stability for several days of varying humidity conditions in the range of 11% to 97%.

A high-performance fully printed flexible humidity sensor was developed using all-carbon-based cellulose nanofiber/graphene nanoplatelet (CNF/GNP) composites as shown in Fig. 4 [43]. The fabricated sensor demonstrated a high (240%) resistive response over the RH range of 30% to 90%, with a fast response time of 17 seconds, and a fast recovery time of 22

seconds. Owing to the abundance, degradability, and biocompatibility of both CNF and GNPs, the results obtained in this study suggest the possibility of fabricating cost-effective and eco-friendly sensors with high performance.

2.4. Smoke sensors

Air pollutants represent a class of the most hazardous pollutants to human beings and animals owing to the toxic effect they pose on skin and eyes, as well as other living tissues [44,45]. Over the past decades, special attention has been given to maintaining the adequate quality of urban air, since air pollution has reached detrimental levels to human health [46]. Unburnt gases such as CO, NO_x, and SO_x are considered the major sources of air pollution [47]. The main sources of these gases include industries, vehicles, aircraft, fumes, and petrochemical plants [48].

In an attempt to avoid false fire alarms that might be activated by non-fire aerosols, Wang S. et al. [49] developed a novel Sauter mean diameter sensor that is based on dual-wavelength technology, instead of smoke concentration, for fire detection. An extra correction channel has been added to the fabricated sensor device to quantify aerosol samples with varying particle sizes and different refractive indices while maintaining a low error of measurement. Results confirmed the ability of the sensor to promptly activate the alarm to fire smoke while avoiding false alarms caused by non-fire aerosols. The developed sensor offers a simple mechanical structure together with high accuracy, improved performance, high sensitivity, and low cost.

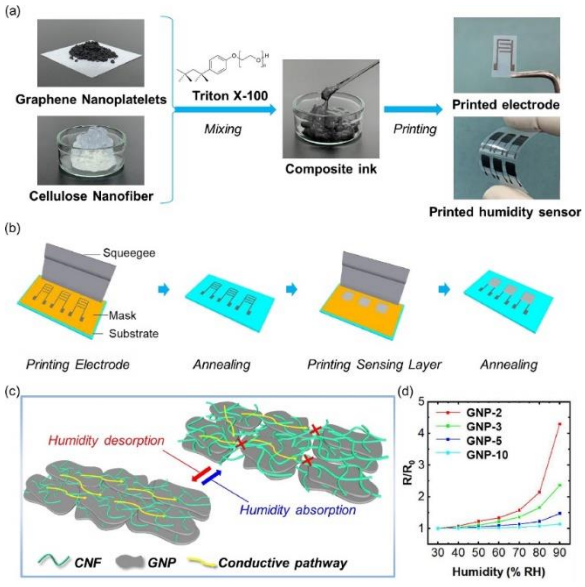

Fig. 4: (a) Fabrication process of CNF/GNP composite inks. (b) The fabrication process of the printed flexible humidity sensors. (c) The sensing mechanism of the CNF/GNP composites humidity sensors. (d) Relative changes in the resistance of the CNF/GNP composites under different humidity conditions. This figure was reproduced with permission from Yoshida et al.[43] (https://creativecommons.org/licenses/by/4.0/)

A smoke sensor, based on Brij 58 functionalized Praseodymium oxide (Pr_6O_{11}) nanostructures, has been fabricated and characterized [50]. Results indicated that in addition to the good crystallinity and optical properties, the Pr_6O_{11} nanomaterials also interestingly demonstrated a significant chromogenic shift, thus acting as efficient smoke sensors. Sensing results confirmed that Pr_6O_{11} nanomaterials demonstrated a significant decrease in the optical absorbance when exposed to smoke, indicating their high affinity to oxidize the smoke gases. They have also successfully decreased CO concentrations by 99%, while those of NO_x and SO_2 gases were 100% eradicated. The results of the proposed sensor system recommend it as an easy, sensitive, and cost-effective system.

A smoke sensor based on a flexible graphene composite has been prepared using Ruddlesden Popper perovskite (RPP) and TiO_2 micro/nanoparticles as sensitizing materials [51]. Electrical characterization measurements showed that RPP microparticle-based sensors had better sensing performance in terms of response and recovery times than those based on TiO_2 nanoparticles. In general, these sensors are favorably characterized by the very low power of 2−7 mW they need to operate, and not needing to be in very close proximity to the source of smoke or fire source as reported in earlier studies. They are also characterized by their fast response time of 1−2 seconds. It can be concluded that these flexible smoke sensors can pave the way to develop a new generation of cost-effective, compact sensors.

Narwade S.H. et al. [52] reported on a highly sensitive and selective room-temperature smoke and humidity sensor based on chemically grown porous hydrangea-type bismuth molybdate (Bi_2MoO_6). To evaluate its performance, the synthesized sensor has been tested against different gases at room temperature (25 ºC). Results demonstrated that under the optimized conditions, the Bi_2MoO_6 sensor showed superior performance for different concentrations of smoke ranging from 5 vol.% up to 40 vol.%, having a sensitive response of 59% towards 40 vol% smoke with a fast response/recovery time of 60/14 seconds at room temperature. In conclusion, the as-obtained Bi_2MoO_6 film sensor presents a considerate repeatability, moderate chemical stability, and substantial mechanical robustness, and despite its n-type semiconducting nature, it still shows a quite good response after exposure to smoke, meaning that it

would have the potential to be used in a fire alarm system.

2.5. Biosensors

Biosensors are devices that comprise a specific receptor molecule to detect the measurand and a physicochemical transducer to generate a measurable signal [53]. Biosensors date back to 1962 when a blood gas-screening biosensor was developed to be used during surgeries [54]. Nowadays, the most frequently used forms of biosensors are home pregnancy tests and glucose detectors, with motivations to introduce new classes of biosensors for a wide range of applications including nucleic acids testing, food analysis, and drug detection [55]. The recent progress in biosensor technology essentially helped in the introduction of novel advanced robust, accurate, and fast-response systems, having the ability to detect changes in analyte levels associated with the presence of a certain disease, thus providing faster diagnosis and, consequently, treatment of many diseases [56].

Huanan G. et al. [57] developed a biosensor composed of a glucose oxidase liposome microreactor (GLM) and glassy carbon electrode (GCE) modified by CS. Cyclic voltammetry (CV) was utilized to study the electrochemical properties of (CS/GLM)n-GCE and pristine GCE and results confirmed that activated glucose oxidase could easily oxidize glucose. Results demonstrated a broad linear range of 0.01–10 mmol/L of glucose. Results also indicated that the activity of electrodes is relatively low (Km=2.35 mmol/L) as obtained by the Michaelis-Menten kinetic model, indicating a better affinity between the enzyme and the substrate. In conclusion, this simple biosensor shows great potential in rapid and inexpensive analysis of glucose, with excellent reproducibility and stability.

A pH biosensor was prepared by Maftoonazad N. and Ramaswamy H. [58] based on an electrospun nanofiber mat of polyvinyl alcohol and a natural pigment from red cabbage extract. Results indicated that the fabricated nanofiber mats are sensitive to changes in pH and can detect pH values in the 2–12 range. Interestingly, results also indicated the reversibility of the colors of the mat corresponding to the changes in the values of pH, highlighting their ability to record transient changes. The sensor's performance was tested on packaged *Rutab* date and its sensing response was perfectly following the changes in the pH of the packaged fruit, meaning that it can record real-time pH-depended changes.

ZnO nanostructures fixed with the antibody of Zika Virus non-structural protein 1 on a printed circuit board were developed and tested as an electrochemical immunosensor [59]. CV measurements were used to assess the sensing performance of the proposed immunosensor. Results confirmed the ability of the developed immunosensor to rapidly detect Zika virus in undiluted urine, with a long linear profile from 0.1 ng/mL up to 100 ng/mL, and a very low limit of detection of less than 1.00 pg/mL. This easy-to-use, lightweight, mobile, and cost-effective immunosensor has great potential for applications in biomedical disciplines.

A molecularly imprinted-based plasmonic biosensor was developed by Safran V. et al. [60] based on Cu^{+2} ions imprinted poly(hydroxyethyl methacrylate-N-metacryloyl-(L)-cysteine methyl ester [PHEMAC-Cu^{+2}] nanoparticles applied to surface Plasmon resonance-based sensor with high selectivity for the detection of Cu^{+2} ions in aqueous solution, Cu^{+2}-spiked artificial urine and physiological serum samples. The affinity of PHEMAC-Cu^{+2} and PHEMAC (control) SPR biosensors was evaluated using the Langmuir adsorption model, and the results demonstrated the homogeneous distribution of Cu^{+2}-sensitive regions on the SPR sensor's surface. In the presence of Zn^{+2} and Ni^{+2} solutions as competitor molecules, the PHEMAC-Cu^{+2} SPR biosensor was more selective towards Cu^{+2} than PHEMAC.

Copper oxide nanoparticles coated with dopamine (CuO@DOP NPs) were synthesized using a facile single-step microwave radiation method [61], as colorimetric and visual fluorescence biosensor for amino acid L-cysteine, which plays a fundamental role in living species. Results indicated the ability of the fabricated sensor to detect L-cysteine with a low detection limit of 0.35 nM. The colorimetric and fluorescence response of the designed sensor was experimentally tested with human blood serum and urine samples, yielding a more than 97% recovery rate of L-cysteine in serum and urine samples, confirming the excellent sensitivity and selectivity of the developed sensor towards L-cysteine under physiological conditions. The as-developed CuO@DOP NPs sensor is deemed practically applicable to provide rapid and selective sensing ability towards L-Cys in different concentrations, with biocompatibility towards the biological systems.

Kaur R. et al. [62] developed a novel bioelectrode based on redox-active protein hemoglobin (Hb) on reduced GO/CS-based biocompatible coatings (ERGO-CS/Hb/FTO), as a quick electrochemical biosensor for methylparathion (MP). Impedimetric measurements demonstrated low charge transfer resistance and solution resistance for the fabricated biosensor, which in turn indicates improved electrochemical performance and sensitivity. The proposed biosensor provided a very low detection limit (79.77 nM) and a high sensitivity of 45.77 Acm^{-2} μM^{-1} with superior reproducibility. It was also found reliable in detecting MP in vegetable samples with a high recovery range of 94%–101%.

A label-free GO-glucose oxidase (GOD)-functionalized long-period fiber grating (LPFG) was designed and presented as a glucose biosensor [63]. The sensing mechanism is based on the reaction

between GOD and glucose which creates gluconic acid and hydrogen peroxide, resulting in a clear shift in the transmission spectrum of LPFG due to the pronounced changes in the refractive index of the surrounding medium. The optimum conditions achieved by the sensor were a 4 mg/mL concentration of GOD and a solution pH of 7. Results showed an excellent linear response of the sensor in the low concentration range (0–1.2 mg/mL) with a sensitivity of ~0.77 nm/(mg/mL), with a fast response speed and shorter response time of 2.16 seconds. In conclusion, the biosensor demonstrated good selectivity and has great potential in the pharmaceutical research and medical diagnosis fields.

An original uric acid biosensor developed using Long-Range Surface Plasmon Resonance (LRSPR) was developed [64]. The proposed biosensor is based on silicon dioxide (SiO_2) as the dielectric layer for the excitation of LRSP modes, owing to its low and tunable refractive index. Sensing results reflect the good response of the LRSPR biosensor to variable concentrations of uric acid ranging from 0.05 mM to 1 mM, with very satisfactory sensitivity of around 21.6°/mM and a low detection limit of 0.02 mM. The practical performance of biosensors was evaluated to detect uric acid in real serum samples and recommended the development of a very sensitive, efficient, cost-effective, and highly selective LRSPR-based biosensor with SiO_2 as a tunable dielectric layer.

Ali M.R. et al. [65] developed a highly sensitive DNA-based electrochemical biosensor for *Vibrio cholerae*. Results revealed high sensitivity of the fabricated biosensor with a long linear range of response to target DNA from 10^{-8} to 10^{-27} mol/L with an excellent detection limit of 7.41 x 10^{-30} mol/L. A selective detection behavior has also been observed. Based on the experimental results, the fabricated biosensor has the potential to be used for six consecutive assays, showing a standard deviation of 5%. Finally, this biosensor offered excellent recovery for the detection of detecting *Vibrio cholerae* in poultry feces, thus qualifying it as a powerful tool for the detection of pathogenic microbes in clinical diagnostics.

An enzyme-free molecularly imprinted impedimetric biosensor for L-hydroxyproline based on 3-aminophenylboronic acid (3-APBA) monomer, and o-phenylenediamine (OPD) has been reported [66]. Results revealed the effect of the structure of the polymer on the charge transfer resistance (R_{ct}) response, indicating that the mixture of monomers resulted in the most pronounced change in R_{ct} due to high selectivity from esterification of 3-APBA and hydrogen bond of OPD. The proposed biosensor indicated that the value R_{ct} increased remarkably upon interaction with L-hydroxyproline, while no change has been recorded in the vale in its absence. The sensor's performance was studied in the range of 0.4–25 μg m/L with a detection limit of 0.13 μg m/L. The performance of the biosensor was also experimentally tested in detecting L-hydroxyproline in human serum samples and yielded satisfactory results.

Molecularly imprinted poly(methacrylic acid) coated on quartz crystal microbalance (QCM) as a highly sensitive and selective biosensor has also been synthesized for the detection of L-tryptophan [67]. Crosslinked by ethylene glycol dimethacrylate, the fabricated sensor demonstrated significant adsorption of approximately 12 mg/g towards L-tryptophan. The sensing experiment was conducted on different concentrations of L-tryptophan, indicating a detection limit of 0.73 ng/mL. The biosensor also demonstrated high selectivity towards L-tryptophan in the presence of D-tryptophan and ascorbic acid. A sensing experiment has also been conducted on real food and urine samples with very high recovery ranging from 97% to 104 %.

Yang B. et al. [68] constructed a graphene/CRISPR-dCas9 electrochemical biosensor for accurate identification of Delta (B.1.617.2), which is one of the most contagious variants of SARS-CoV-2 virus which causes COVID-19. The signal detected by the biosensor is amplified by a [Ru(phen)2dppz]BF4-based probe. Results indicated that this clinical diagnostic method could deliver the results totally within 47 minutes. Results indicated a 1.2 pM limit of detection with very acceptable reproducibility. Results also indicated that the biosensor showed satisfactory selectivity for Delta among other variances of SARS-CoV-2 such as Alpha, Beta, and Gamma. 26 real clinical samples were used for further validation of this detection assay, indicating 100% of both clinical sensitivity and clinical specificity, leading to the conclusion that this biosensor could provide a reliable diagnostic assay for identifying SARS-CoV-2 variants.

Another SARS-CoV-2 biosensor has also been developed by [69] using electronic labeling of protein molecules and employing colloidal quantum dots (CQDs)-modified electrodes. Results confirmed the detection of the characteristic peak resulting from the interaction between the SARS-CoV-2 antigen and antibody, which is detected by the CQDs-modified electrode. The performance of the proposed biosensor has been also tested on real serum specimens from COVID-19 patients, reflecting its ability to quantify SARS-CoV-2 antibodies with a 93.8% correlation coefficient when compared to the ELISA test. Results also demonstrated the ability of the biosensor to discriminate between COVID-19 and normal samples with an accuracy of around 90%.

3. Molecular modeling approaches

Molecular modeling and other computational simulation methods have proved their capabilities in studying the properties and interactions between different chemical structures and provide reliable data concerning all biological, chemical, and physical features [70-75]. QSAR methodology is a computational tool that can quantify the relationship between a certain biological structure's physicochemical properties and its biological activities [76-78]. Furthermore, there is another valuable concept in molecular modeling calculations that offers entirely accurate information on several chemical entities' effective sites. This concept is known as Molecular Electrostatic Potential (MESP). It is also critical in estimating the chemical addition nature through which a chemical structure is most possible to go through, either the electrophilic or nucleophilic chemical addition. Molecular modeling is generally widely applied to study the structural, thermal, and vibrational features of many molecules [79-83]. Physical properties such as MESP, total dipole moment, and HOMO/LUMO bandgap energy reflect the studied structures' reactivity [84-87]. Accordingly, these parameters are calculated as a descriptor for the reactivity of the studied structures.

For a given surface to be an active surface for sensing experiment modeling data could suggest how can one modify the surface based on the physical descriptor while QSAR could be a good descriptor for a given surface to act as a biosensor.

Applying these concepts one can find many authors applying different levels of theory to apply the given structure as sensors.

Modeling data suggested that modified biopolymers with nano metal oxide such as TiO_2 could act as efficient biosensors for amino acids [88]. It is also stated that fullerene shows abilities to be a gas sensor for harmful gases such as halides [89]. Molecular modeling supports the experimental findings that, nano-modified Polyaniline is sensitive to formaldehyde [90]. Molecular modeling could also confirm the experimental data which stated that graphene foam decorated with ZnO could be applied as a humidity sensor [91]. Modeling at a higher level of theory indicated that, some polymer blends such as Polyvinyl alcohol/Polypropylene enhanced with nano ZnO showed surface activity to be applied as gas sensors [92]. Finally, Graphene modified with Nickel Oxide shows the ability to act as a humidity sensor [93].

4. Recent approaches

Recently, corrodes are devolved as an ion sensor. It is stated that corroles have been vastly utilized in the field of biology, medicine, environment, photophysics, etc. Sensing the hazardous metal ions being one of the most important applications of corroles has rendered fruitful results in biological and environmental sciences [94-100].

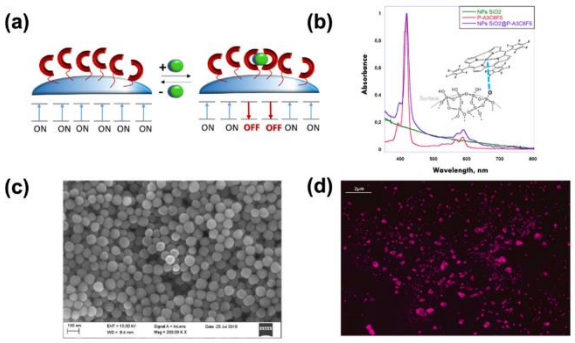

Fig. 5: (a) Illustration of the dye–dye interaction's effect of Phosphorous (V) Corrole Fluorophores-functionalized SiO_2 nanoparticles (SiO_2NPs@PFCorr), on nitrite ion sensitivity; (b) the UV-vis spectrum; (c) SEM; and (d) the optical fluorescent microscopy images of SiO_2NPs@PFCorr hybrid assemblies. This figure was reproduced with permission from Caroleo et al.[98] (https://creativecommons.org/licenses/by/4.0/)

5. Conclusions and Perspectives

Sensor development is among the most demanded technologies to meet the requirements of everyday life in different fields and disciplines. Recent advances in sensor technology are directed toward synthesizing /using smart materials and utilizing different spectroscopic, electrical, optical, and chemical techniques to assess the performance of the fabricated sensors. This review presented the recent advances in the development and performance of gas, humidity, temperature, and smoke sensors, and biosensors implemented in different fields of application. Continued progress in sensor technology via the introduction of new application-specific cost-effective sensing materials, improvement of the fabrication methods, and enhancing sensors' performance is required and is eventually beneficial.

6. Conflicts of interest

There are no conflicts to declare.

7. Formatting of funding sources

No funding for this work.

8. Acknowledgments

We sincerely thank the organizing committee of The Fourth Hybrid International Conference on Molecular Modeling and Spectroscopy for the immense support and encouragement to carry out this work.

9. References

[1] K. Kalantar-zadeh, Sensors: An Introductory Course, Springer US, Boston, MA, USA 2013, pp. 11–28.

[2] C. Dincer, R. Bruch, E. Costa-Rama, M.T. Fernández-Abedul, A. Merkoçi, A. Manz, G.A. Urban, F. Güder, Disposable Sensors in Diagnostics, Food, and Environmental Monitoring, *Adv. Mater.* **31**(30), 1806739 (2019). https://doi.org/10.1002/adma.201806739

[3] H.-R. Tränkler, O. Kanoun, "Recent Advances in Sensor Technology", in Proceedings of the 18th IEEE Instrumentation and Measurement Technology Conference (IMTC), vol. 1, May 2001, pp. 309-316. https://doi.org/10.1109/IMTC.2001.928831

[4] M. Javaid, A. Haleem, S. Rab, R.P. Singh, R. Suman, Sensors for daily life: A review, *Sensors International* **2**, 100121 (2021). https://doi.org/10.1016/j.sintl.2021.100121

[5] H. Elhaes, A. Fakhry, M. Ibrahim, Carbon nano materials as gas sensors, *Mater Today-Proc.* **3**, 2483–2492 (2016). https://doi.org/10.1016/j.matpr.2016.04.166

[6] A. Mirzaei, J.-H. Kim, H.W. Kima, S.S. Kim, How shell thickness can affect the gas sensing properties of nanostructured materials: Survey of literature, *Sensor Actuat. B-Chem.* **258**, 270-294 (2018). https://doi.org/10.1016/j.snb.2017.11.066

[7] T. Singh, U. Bonne, Gas Sensors. Reference Module in Materials Science and Materials Engineering, Elsevier, 2017. https://doi.org/10.1016/B978-0-12-803581-8.00548-8

[8] S. Touba, S. Kimiagar, Enhancement of sensitivity and selectivity of α-Fe_2O_3 nanorod gas sensors by ZnO nanoparticles decoration, *Mat. Sci. Semicon. Proc.* **102**, 104603 (2019). https://doi.org/10.1016/j.mssp.2019.104603

[9] N. Zubair, K. Akhtar, High performance room temperature gas sensor based on novel morphology of zinc oxide nanostructures, *Trans. Nonferrous Met. Soc. China* **29**, 143−156 (2019). https://doi.org/10.1016/S1003-6326(18)64923-4

[10] S.B. Kulkarni, Y.H. Navale, S.T. Navale, F.J. Stadler, N.S. Ramgir, V.B. Patil, Hybrid Polyaniline-WO_3 Flexible Sensor: A Room Temperature Competence Towards NH_3 Gas, *Sensor Actuat. B-Chem.* **288**, 279-288 (2019). https://doi.org/10.1016/j.snb.2019.02.094

[11] M.O. Diniz, A.F. Golin, M.C. Santos, R.F. Bianchi, E.M. Guerra, Improving performance of polymer-based ammonia gas sensor using POMA/V_2O_5 hybrid films, *Org. Electron.* **67**, 215–221 (2019). https://doi.org/10.1016/j.orgel.2019.01.039

[12] R. Abdelghani, H.S. Hassan, I. Morsi, A.B. Kashyout, Nano-architecture of highly sensitive SnO_2–based gas sensors for Acetone and Ammonia using Molecular Imprinting Technique, *Sensor Actuat. B-Chem.* **297**, 126668 (2019). https://doi.org/10.1016/j.snb.2019.126668

[13] S.A.M. Chachuli, M.N. Hamidon, M.S. Mamat, M. Ertugrul, N.H. Abdullah, Response of TiO_2/MWCNT/B_2O_3 gas sensor to hydrogen using different organic binder, *Mat. Sci. Semicon. Proc.* **99**, 140–148 (2019). https://doi.org/10.1016/j.mssp.2019.04.009

[14] N.L. Myadam, D.Y. Nadargi, J.D.G. Nadargi, F.I. Shaikh, S.S. Suryavanshi, M.G. Chaskar, A facile approach of developing Al/SnO_2 xerogels via epoxide assisted gelation: A highly versatile route for formaldehyde gas sensors, *Inorg. Chem. Commun.* **116**, 107901 (2020). https://doi.org/10.1016/j.inoche.2020.107901

[15] Z. Gao, G. Song, X. Zhang, Q. Li, S. Yang, T. Wang, Y. Li, L. Zhang, L. Guo, Y. Fu, A facile PDMS coating approach to room-temperature gas sensors with high humidity resistance and long-term stability, *Sensor Actuat. B-Chem.* **325**, 128810 (2020). https://doi.org/10.1016/j.snb.2020.128810

[16] N. Kohli, A. Hastir, M. Kumari, R.C. Singh, Hydrothermally synthesized heterostructures of In_2O_3/MWCNT as acetone gas sensor, *Sensor Actuat. A-Phys.* **314**, 112240 (2020). https://doi.org/10.1016/j.sna.2020.112240

[17] N.M. Santhosh, A. Vasudevan, A. Jurov, A. Korent, P. Slobodian, J. Zavašnik, U. Cvelbar, Improving sensing properties of entangled carbon nanotube-based gas sensors by atmospheric plasma surface treatment, *Microelectron. Eng.* **232**, 111403 (2020). https://doi.org/10.1016/j.mee.2020.111403

[18] S.N.A. Mustaffa, N.A. Ariffin, A.L. Khalaf, M.H. Yaacob, N. Tamchek, S. Paiman, S. Sagadevan, Sensing mechanism of an optimized room temperature optical hydrogen gas sensor made of zinc oxide thin films, *J. Mater. Res. Technol.* **9**(5), 10624–10634 (2020). https://doi.org/10.1016/j.jmrt.2020.07.086

[19] N.T. Vinh, L.A. Tuan, L.K. Vinh, N.V. Quy, Synthesis, characterization, and gas sensing properties of Fe_3O_4/FeOOH nanocomposites for a mass-type gas sensor, *Mat. Sci. Semicon. Proc.* **118**, 105211 (2020). https://doi.org/10.1016/j.mssp.2020.105211

[20] I. Strauss, K. Chakarova, A. Mundstock, M. Mihaylov, K. Hadjiivanov, N. Guschanski, J. Caro, UiO-66 and UiO-66-NH_2 based sensors: Dielectric and FTIR investigations on the effect of CO_2 adsorption, *Micropor. Mesopor. Mat.* **302**, 110227 (2020). https://doi.org/10.1016/j.micromeso.2020.110227

[21] A. Umar, A.A. Ibrahim, H. Algadi, H. Albargi, M.A. Alsairi, Y. Wang, S. Akbar, Enhanced NO_2 Gas Sensor Device based on supramolecularly assembled polyaniline/silver oxide/graphene oxide composites,

Ceram. Int. **47**(18), 25696-25707 (2021). https://doi.org/10.1016/j.ceramint.2021.05.296
[22] B. Salah, A.I. Ayesh, Fabrication of H_2S sensitive gas sensors formed of SnO_2–Fe_2O_3 composite nanoparticles, *Mater. Chem. Phys.* **266**, 124597 (2021). https://doi.org/10.1016/j.matchemphys.2021.124597
[23] G.J. Thangamani, S.K. Khadheer Pasha, Titanium dioxide (TiO_2) nanoparticles reinforced polyvinyl formal (PVF) nanocomposites as chemiresistive gas sensor for sulfur dioxide (SO_2) monitoring, *Chemosphere* **275**, 129960 (2021). https://doi.org/10.1016/j.chemosphere.2021.129960
[24] J.G. Thangamani, S.K. Khadheer Pasha, Hydrothermal synthesis of copper (II) oxide-nanoparticles with highly enhanced BTEX gas sensing performance using chemiresistive sensor, *Chemosphere* **277**, 130237 (2021). https://doi.org/10.1016/j.chemosphere.2021.130237
[25] A. Sholehah, K. Karmala, N. Huda, L. Utari, N.L.W. Septiani, B. Yuliarto, Structural effect of ZnO-Ag chemoresistive sensor on flexible substrate for ethylene gas detection, *Sensor Actuat. A-Phys.* **331**, 112934 (2021). https://doi.org/10.1016/j.sna.2021.112934
[26] K. Drozdowska, T. Welearegay, L. Österlund, J. Smulko, Combined chemoresistive and in *situ* FTIR spectroscopy study of nanoporous NiO films for light-activated nitrogen dioxide and acetone gas sensing, *Sensor Actuat. B-Chem.* **353**, 131125 (2022). https://doi.org/10.1016/j.snb.2021.131125
[27] H. Kumar, N. Kumari, D. Singh, Quantum dots decorated polyaniline plastic nanocomposites as a novel amperometric sensor for formaldehyde: Experimental and theoretical approach, *Talanta Open* **6**, 100141 (2022). https://doi.org/10.1016/j.talo.2022.100141
[28] H.Y. Mohammed, M.A. Farea, P.W. Sayyad, N.N. Ingle, T. Al-Gahouari, M.M. Mahadik, G.A. Bodkhe, S.M. Shirsat, M.D. Shirsat, Selective and sensitive chemiresistive sensors based on polyaniline/graphene oxide nanocomposite: A cost-effective approach, *Journal of Science: Advanced Materials and Devices* **7**, 100391 (2022). https://doi.org/10.1016/j.jsamd.2021.08.004
[29] A. Umar, A.A. Ibrahim, H. Algadi, H. Albargi, M.A. Alsairi, Y. Wang, S. Akbar, Supramolecularly assembled isonicotinamide/reduced graphene oxide nanocomposite for room-temperature NO_2 gas sensor, *Environmental Technology & Innovation* **25**, 102066 (2022). https://doi.org/10.1016/j.eti.2021.102066
[30] I.S. Elashmawi, A.M. Abdelghany, & N.A. Hakeem, N. A. (2013). Quantum confinement effect of CdS nanoparticles dispersed within PVP/PVA nanocomposites. *Journal of Materials Science: Materials in Electronics*, 24, 2956-2961 (2013). https://doi.org/10.1007/s10854-013-1197-z
[31] M. Nitani, K. Nakayama, M. Kazuki, M. Omori, M. Uno, Organic temperature sensors based on conductive polymers patterned by a selective-wetting method, *Org. Electron.* **71**, 164-168 (2019). https://doi.org/10.1016/j.orgel.2019.05.006
[32] V. Kumar, J. Verma, A.S. Maan, J. Akhtar, Epitaxial 4H–SiC based Schottky diode temperature sensors in ultra-low current range, *Vacuum* **182**, 109590 (2020). https://doi.org/10.1016/j.vacuum.2020.109590
[33] Y. Liu, L.B. Yuan Ultrasensitive temperature sensor based on a urethane acrylate-coated off-axis spiral long period fiber grating, *Optik - International Journal for Light and Electron Optics* **223**, 165557 (2020). https://doi.org/10.1016/j.ijleo.2020.165557
[34] S. Qiu, J. Yuan, S. Duan, X. Zhou, C. Mei, Y. Qu, B. Yan, Q. Wu, K. Wang, X. Sang, K. Long, C. Yu, High sensitivity temperature sensor based on a helically twisted photonic crystal fiber, *Results Phys.* **29**, 104767 (2021). https://doi.org/10.1016/j.rinp.2021.104767
[35] S. Liu, G. Lu, D. Lv, M. Chen, Z. Zhang, Sensitivity enhanced temperature sensor with cascaded Sagnac loops based on harmonic Vernier effect, *Opt. Fiber Technol.* **66**, 102654 (2021). https://doi.org/10.1016/j.yofte.2021.102654
[36] X. Wang, B. Mu, L. Zhang, X. Zhang, Drift characteristic analysis of additive manufactured Ag NPs-PEDOT:PSS flexible temperature sensor, *Results in Engineering* **13**, 100384 (2022). https://doi.org/10.1016/j.rineng.2022.100384
[37] M. Schepperle, M. Ghanam, A. Bucherer, T. Gerach, P. Woias, Noninvasive platinum thin-film microheater/temperature sensor array for predicting and controlling flow boiling in microchannels, *Sensor Actuat. A-Phys.* **345**, 113811 (2022). https://doi.org/10.1016/j.sna.2022.113811
[38] H.-S. Kim, J.H. Kim, S.-Y. Park, J.-H. Kang, S.-J. Kim, Y.-B. Choi, U.S. Shin, Carbon nanotubes immobilized on gold electrode as an electrochemical humidity sensor, *Sensor Actuat. B-Chem.* **300**, 127049 (2019). https://doi.org/10.1016/j.snb.2019.127049
[39] Z. Wang, Y. Zhang, W. Wang, Q. An, W. Tong, High performance of colorimetric humidity sensors based on minerals, *Chem. Phys. Lett.* **727**, 90–94 (2019). https://doi.org/10.1016/j.cplett.2019.04.066
[40] X. Zhao, X. Chen, X. Yu, X. Ding, X. Yu, K. Tang, High Sensitivity Humidity Sensor and Its Application in Nondestructive Testing for Wet Paper, *Sensor Actuat. B-Chem.* **301**, 127048 (2019). https://doi.org/10.1016/j.snb.2019.127048
[41] C. Zhu, L.-Q. Tao, Y. Wang, K. Zheng, J. Yu, L. Xiandong, X. Chen, Y. Huang, Graphene oxide humidity sensor with laser-induced graphene porous electrodes, *Sensor Actuat. B-Chem.* **325**, 128790 (2020). https://doi.org/10.1016/j.snb.2020.128790

[42] M.F. de Aguiar, A.N.R. Leal, C.P. de Melo, K.G.B. Alves, Polypyrrole-coated electrospun polystyrene films as humidity sensors, *Talanta* **234**, 122636 (2021). https://doi.org/10.1016/j.talanta.2021.122636

[43] A. Yoshida, Y.-F. Wang, S. Tachibana, A. Hasegawa, T. Sekine, Y. Takeda, J. Hong, D. Kumaki, T. Shiba, S. Tokito, Printed, all-carbon-based flexible humidity sensor using a cellulose nanofiber/graphene nanoplatelet composite, *Carbon Trends* **7**, 100166 (2022). https://doi.org/10.1016/j.cartre.2022.100166

[44] D.E. Jorenby, S.S. Smith, M.C. Fiore, T.B. Baker, Nicotine levels, withdrawal symptoms, and smoking reduction success in real world use: A comparison of cigarette smokers and dual users of both cigarettes and E-cigarettes, *Drug Alcohol Depend.* **170**, 93–101 (2017). https://doi.org/10.1016/j.drugalcdep.2016.10.041

[45] R.S. Mwiru, T.J. Nagu, P. Kaduri, F. Mugusi, W. Fawzi, Prevalence and patterns of cigarette smoking among patients co-infected with human immunodeficiency virus and tuberculosis in Tanzania, *Drug Alcohol Depend.* **170**, 128–132 (2017). https://doi.org/10.1016/j.drugalcdep.2016.11.006.

[46] S. Squizzato, M. Cazzaro, E. Innocente, F. Visin, P.K. Hopke, G. Rampazzo, Urban air quality in a mid-size city- PM2.5 composition, sources and identification of impact areas: From local to long range contributions, *Atmos. Res.* **186**, 51–62 (2017). https://doi.org/10.1016/j.atmosres.2016.11.011

[47] A.G. Alsultan, N.A. Mijan, N. Mansir, S.Z. Razali, R. Yunus, Y.H. Taufiq-Yap, Combustion and Emission Performance of CO/NO_x/SO_x for Green Diesel Blends in a Swirl Burner, *ACS Omega* **6**(1), 408–415 (2021). https://doi.org/10.1021/acsomega.0c04800

[48] S.A. Qamar, P. Bhatt, S. Ghotekar, M. Bilal, Nanomaterials for bioremediation of air pollution. In Iqbal H.M.N., Bilal M., Nguyen T.A. (Eds.), *Micro and Nano Technologies, Nano-Bioremediation: Fundamentals and Applications* (pp. 243–261), Elsevier (2022). https://doi.org/10.1016/B978-0-12-823962-9.00008-8

[49] S. Wang, X. Xiao, T. Deng, A. Chen, M. Zhu, A Sauter mean diameter sensor for fire smoke detection, *Sensor Actuat. B-Chem.* **281**, 920–932 (2019). https://doi.org/10.1016/j.snb.2018.11.021

[50] P. Sharma, S. Chaudhary, R. Kumar, A. Umar, Smoke sensing applications of Brij 58 functionalized Praseodymium oxide (Pr_6O_{11}) nanostructures, *Sensor Actuat. B-Chem.* **297**, 126628 (2019). https://doi.org/10.1016/j.snb.2019.126628

[51] A.I. Mtz-Enriquez, K.P. Padmasree, A.I. Oliva, C. Gomez-Solis, E. Coutino-Gonzalez, C.R. Garcia, D. Esparza, J. Oliva, Tailoring the detection sensitivity of graphene based flexible smoke sensors by decorating with ceramic microparticles, *Sensor Actuat. B-Chem.* **305**, 127466 (2020). https://doi.org/10.1016/j.snb.2019.127466

[52] S.H. Narwade, P.V. Shinde, N.M. Shinde, V.V. Jadhav, S.F. Shaikh, R.S. Mane, U.V. Bhosle, Hydrangea-type bismuth molybdate as a room-temperature smoke and humidity sensor, *Sensor Actuat. B-Chem.* **348**, 130643 (2021). https://doi.org/10.1016/j.snb.2021.130643

[53] V.R. Samuel, K.J Rao, A review on label free biosensors, *Biosensors and Bioelectronics: X*. **11**, 100216 (2022). https://doi.org/10.1016/j.biosx.2022.100216

[54] L.C. Clark, C. Lyons, Electrode systems for continuous monitoring in cardiovascular surgery, *Ann. N. Y. Acad. Sci.* **102**, 29–45 (1962). https://doi.org/10.1111/j.1749-6632.1962.tb13623.x

[55] A. Michelmore, Thin film growth on biomaterial surfaces. In *Thin Film Coatings for Biomaterials and Biomedical Applications* (pp. 29–47), Woodhead Publishing (2016). https://doi.org/10.1016/B978-1-78242-453-6.00002-X

[56] N.M. Noah, P.M. Ndangili, Green synthesis of nanomaterials from sustainable materials for biosensors and drug delivery, *Sensors International* **3**, 100166 (2022). https://doi.org/10.1016/j.sintl.2022.100166

[57] G. Huanan, G. Dezhuang, S. Yan, H. Bolin, Z. Na, Biosensor composed of integrated glucose oxidase with liposome microreactors/chitosan nanocomposite for amperometric glucose sensing, *Colloid Surface A* **574**, 260–267 (2019). https://doi.org/10.1016/j.colsurfa.2019.04.076

[58] N. Maftoonazad, H. Ramaswamy, Design and testing of an electrospun nanofiber mat as a pH biosensor and monitor the pH associated quality in fresh date fruit (*Rutab*), *Polym. Test* **75**, 76–84 (2019). https://doi.org/10.1016/j.polymertesting.2019.01.011

[59] A.M. Faria, T. Mazon, Early diagnosis of Zika infection using a ZnO nanostructures-based rapid electrochemical biosensor, *Talanta* **203**, 153-160 (2019). https://doi.org/10.1016/j.talanta.2019.04.080

[60] V. Safran, I. Göktürk, A. Derazshamshir, F. Yılmaz, N. Sağlam, A. Denizli, Rapid sensing of Cu^{+2} in water and biological samples by sensitive molecularly imprinted based plasmonic biosensor, *Microchem. J.* **148**, 141-150 (2019). https://doi.org/10.1016/j.microc.2019.04.069

[61] D. Rohilla, S. Chaudhary, N. Kaur, A. Shanavas, Dopamine functionalized CuO nanoparticles: A high valued "turn on" colorimetric biosensor for detecting cysteine in human serum and urine samples, *Mat. Sci. Eng. C-Mater.* **110**, 110724 (2020). https://doi.org/10.1016/j.msec.2020.110724

[62] R. Kaur, S. Rana, K. Lalit, P. Singh, K. Kaur, Electrochemical detection of methyl parathion via a novel biosensor tailored on highly biocompatible electrochemically reduced graphene oxide-chitosan-haemoglobin coatings, *Biosensors and Bioelectronics* **167**, 112486 (2020). https://doi.org/10.1016/j.bios.2020.112486

[63] B. Xu, J. Huang, L. Ding, J. Cai, Graphene oxide-functionalized long period fiber grating for ultrafast label-free glucose biosensor, *Mat. Sci. Eng. C-Mater.* **107**, 110329 (2020). https://doi.org/10.1016/j.msec.2019.110329

[64] S. Jain, A. Paliwal, V. Gupta, M. Tomar, Refractive index tuning of SiO_2 for Long Range Surface Plasmon Resonance based biosensor, *Biosensors and Bioelectronics* **168**, 112508 (2020). https://doi.org/10.1016/j.bios.2020.112508

[65] M.R. Ali, M.S. Bacchu, M.A.A. Setu, S. Akter, M.N. Hasan, F.T. Chowdhury, M.M. Rahman, M.S. Ahommed, M.Z.H. Khan, Development of an advanced DNA biosensor for pathogenic *Vibrio cholerae* detection in real sample, *Biosensors and Bioelectronics* **188**, 113338 (2021). https://doi.org/10.1016/j.bios.2021.113338

[66] W. Jesadabundit, S. Jampasa, K. Patarakul, W. Siangproh, O. Chailapakul, Enzyme-free impedimetric biosensor-based molecularly imprinted polymer for selective determination of L-hydroxyproline, *Biosensors and Bioelectronics* **191**, 113387 (2021). https://doi.org/10.1016/j.bios.2021.113387

[67] K. Prabakaran, P.J. Jandas, J. Luo, C. Fu, Q. Wei, Molecularly imprinted poly(methacrylic acid) based QCM biosensor for selective determination of L-tryptophan, *Colloid Surface A* **611**, 125859 (2021). https://doi.org/10.1016/j.colsurfa.2020.125859

[68] B. Yang, X. Zeng, J. Zhang, J. Kong, X. Fang, Accurate identification of SARS-CoV-2 variant delta using graphene/CRISPR-dCas9 electrochemical biosensor, *Talanta* **249**, 123687 (2022). https://doi.org/10.1016/j.talanta.2022.123687

[69] Y. Zhao, J. Chen, Z. Hu, Y. Chen, Y. Tao, L. Wang, L. Li, P. Wang, H.-Y. Li, J. Zhang, J. Tang, H. Liu, All-solid-state SARS-CoV-2 protein biosensor employing colloidal quantum dots-modified electrode, *Biosensors and Bioelectronics* **202**, 113974 (2022). https://doi.org/10.1016/j.bios.2022.113974

[70] M. Ibrahim, N. Saleh, W. Elshemey, A. Elsayed, Hexapeptide functionality of cellulose as NS3 protease inhibitors, *Med. Chem.* **8**, 826-830 (2012). https://doi.org/10.2174/157340612802084144

[71] E.A. Assirey, S.M. Sirry, H.A. Burkani, M.A. Ibrahim, Modified Ziziphus spina-christi stones as green route for the removal of heavy metals, *Sci. Rep.* **10**, 20557 (2020). https://doi.org/10.1038/s41598-020-76810-y

[72] R.S. Saji, J.C. Prasana, S. Muthu, J. George, T.K. Kuruvilla, B.R. Raajaraman, Spectroscopic and quantum computational study on naproxen sodium, *Spectrochim. Acta A* **226**, 117614 (2020). https://doi.org/10.1016/j.saa.2019.117614

[73] L. Dinparast, S. Hemmati, A.A. Alizadeh, G. Zengin, H.S. Kafil, M.B. Bahadori, S. Dastmalchi, An efficient, catalyst-free, one-pot synthesis of 4H-chromene derivatives and investigating their biological activities and mode of interactions using molecular docking studies, *J. Mol. Struct.* **1203**, 127426 (2020). https://doi.org/10.1016/j.molstruc.2019.127426

[74] H. Ezzat, A.A. Menazea, W. Omara, O.H. Basyouni, S.A. Helmy, A.A. Mohamed, W. Tawfik, M. Ibrahim, DFT:B3LYP/LANL2DZ Study for the Removal of Fe, Ni, Cu, As, Cd and Pb with Chitosan, *Biointerface Res. Appl. Chem.* **10**, 7002–7010 (2020), https://doi.org/10.33263/BRIAC106.70027010

[75] A. Refaat, M.A. Ibrahim, H. Elhaes, R. Badry, H. Ezzat, I.S. Yahia, H.Y. Zahran, M. Shkir, Geometrical, vibrational, and physical properties of polyvinyl chloride nanocomposites: Molecular Modeling Approach, *J. Theor. Comput. Chem.*, **18**(8), 1950037 (2019). https://doi.org/10.1142/S0219633619500378

[76] N.A. Saleh, H. Elhaes, M. Ibrahim, Design and development of some viral protease inhibitors by QSAR and molecular modeling studies. In: Viral proteases and their inhibitors. 1st Edition, pp. 25-58, Elsevier (2017). https://doi.org/10.1016/B978-0-12-809712-0.00002-2

[77] F.A. Bulat, A. Toro-Labbé, T. Brinck, J.S. Murray, P. Politzer, Quantitative analysis of molecular surfaces: areas, volumes, electrostatic potentials and average local ionization energies, *Journal of Molecular Modeling* 16, 1679-1691 (2010), https://doi.org/10.1007/s00894-010-0692-x

[78] A.M. Fahim, M.A. Shalaby, M.A. Ibrahim, Microwave-assisted synthesis of novel 5-aminouracil-based compound with DFT calculations, *J. Mol. Struct.* **1194**, 211-226 (2019), https://doi.org/10.1016/j.molstruc.2019.04.078

[79] A.A. Mahmoud, O. Osman, H. Elhaes, M. Ferretti, A. Fakhry, M.A. Ibrahim, Computational Analyses for the Interaction Between Aspartic Acid

and Iron, *J. Comput. Theor. Nanosci.* **15**, 470-473 (2018). https://doi.org/10.1166/jctn.2018.7113
[80] M.A. El-Mansy, A.M. Bayoumy, H. Ezzat, N. El-Sayed, H. Elhaes, M.A. Ibrahim, Modeling the Effect of Hydration on the Electronic and Vibrational Properties of AZT. *Biointerface Res. Appl. Chem.* **11**, 9253-9265 (2021). https://doi.org/10.33263/briac112.92539265
[81] A.M.F. Galal, D. Atta, A. Abouelsayed, M.A. Ibrahim, A.G. Hanna, Configuration and molecular structure of 5-chloro-N-(4-sulfamoylbenzyl) salicylamide derivatives. *Spectrochim. Acta A* **214**, 476-486 (2019). https://doi.org/10.1016/j.saa.2019.02.070
[82] A. El-Barbary, M. El-Nahass, M. Kamel, M.A.M. El-Mansy, FT-IR, FT-Raman spectra and ab initio HF, DFT vibrational analysis of P-methyl acetanilide, *Journal of Applied Sciences Research* **5**(11), 1977-1987 (2009).
[83] M. El-Mansy, M. El-Bana, S. Fouad, On the spectroscopic analyses of 3-Hydroxy-1-Phenyl-Pyridazin-6 (2H) one (HPHP): A comparative experimental and computational study. *Spectrochim. Acta Part A* **176**, 99-105 (2017). https://doi.org/10.1016/j.saa.2016.12.040
[84] M. Ibrahim, H. El-Haes Computational Spectroscopic Study of Copper, Cadmium, Lead and Zinc Interactions in the Environment, *Int. J. Environ. Pollut.* **23**, 417-424 (2005), https://doi.org/10.1504/IJEP.2005.007604
[85] M. Ibrahim, A.A. Mahmoud, Computational Notes on the Reactivity of some Functional Groups, *J. Comput. Theor. Nanosci.* **6**, 1523-1526 (2009). https://doi.org/10.1166/jctn.2009.1205
[86] P. Politzer, P.R. Laurence, K. Jayasuriya, Molecular electrostatic potentials: an effective tool for the elucidation of biochemical phenomena, *Environ. Health Persp.* **61**, 191-202 (1985), https://doi.org/10.1289/ehp.8561191
[87] Z.S. Şahin, H.I. Şenöz, H. Tezcan, O. Büyükgüngör, Synthesis, spectral analysis, structural elucidation and quantum chemical studies of (E)-methyl-4-[(2-phenylhydrazono)methyl]benzoate, *Spectrochim. Acta A* **143**, 91-100 (2015). https://doi.org/10.1016/j.saa.2015.02.032
[88] M. Ibrahim, A.-A. Mahmoud, O. Osman, A. Refaat, E. M. El-Sayed, Molecular Spectroscopic Analyses of Nano Chitosan Blend as Biosensor, *Spectrochim. Acta Part A.* **77**, 802-806 (2010). https://doi.org/10.1016/j.saa.2010.08.007
[89] H. Elhaes, M. Ibrahim, Fullerene as Sensor for Halides: Modeling Approach, *J. Comput. Theor. Nanosci.* **10**, 2026-2028 (2013). https://doi.org/10.1166/jctn.2013.3164
[90] W. Omara, R. Amin, H. Elhaes, M. Ibrahim, S.A. Elfeky, Preparation and Characterization of Novel Polyaniline Nanosensor for Sensitive Detection of Formaldehyde, *Recent Pat. Nanotechnol.* **9**(3), 195-203 (2015). https://doi.org/10.2174/1872210510999151126112509
[91] M. Morsy, M. Ibrahim, Z. Yuan, F. Meng, Graphene foam decorated with ZnO as a humidity sensor, IEEE Sensors Journal, **20**(4), 1721-1729 (2020). https://doi.org/10.1109/JSEN.2019.2948983
[92] R. Badry, A. Fahmy, A. Ibrahim, H. Elhaes, M. Ibrahim, Application of Polyvinyl alcohol/Polypropylene/Zinc Oxide Nanocomposites as Sensor: Modeling Approach, *Opt. Quant. Electron.* **53**, 39 (2021). https://doi.org/10.1007/s11082-020-02646-5
[93] A.M. Bayoumy, I. Gomaa, H. Elhaes, M. Selim, M.A. Ibrahim, Application of Graphene/Nickel Oxide Composite as a Humidity Sensor, *Egypt. J. Chem.* **64**(1), 85-91 (2021). https://doi.org/10.21608/ejchem.2020.36453.2753
[94] G. Lu, P. Zhang, Y. Gao, S. Yu, Y. Yang, Preparation and third order nonlinear optical properties of corrole functionalized GO nanohybrids, *Opt Laser. Technol.* 149, 107813 (2022). https://doi.org/10.1016/j.optlastec.2021.107813
[95] I. Yadav, D. Dhiman, M. Sankar, β-Disubstituted silver (III) corroles: facile synthesis, photophysical and electrochemical redox properties, *J. Porphyr. Phthalocyanines* **25**(05n06), 547-554 (2021). https://doi.org/10.1142/S1088424621500437
[96] M. Rezazadeh, S. Seidi, M. Lid, S. Pedersen-Bjergaard, Y. Yamini, The modern role of smartphones in analytical chemistry, *TrAC, Trends Anal. Chem.* **118**, 548-555 (2019). https://doi.org/10.1016/j.trac.2019.06.019
[97] R. Paolesse, S. Nardis, D. Monti, M. Stefanelli, C. Di Natale, Porphyrinoids for chemical sensor applications, *Chem. Rev.* **117**(4), 2517-2583 (2017). https://doi.org/10.1021/acs.chemrev.6b00361
[98] F. Caroleo, G. Diedenhofen, A. Catini, C. Di Natale, R. Paolesse, L. Lvova, Phosphorous (V) corrole fluorophores for nitrite assessment in environmental and biological samples, *Chemosensors* **10**(3), 107 (2022). https://doi.org/10.3390/chemosensors10030107
[99] G. Lu, Y. Gao, X. Wang, D. Zhang, S. Meng, S. Yu, Y. Zhuang, A corrole-based fluorescent probe for detection of sulfur ion and its application in living cells, *Dyes Pigm.* **197**, 109941 (2022). https://doi.org/10.1016/j.dyepig.2021.109941
[100] L. Lvova, G. Pomarico, F. Mandoj, F. Caroleo, C. Di Natale, K.M. Kadish, S. Nardis Smartphone coupled with a paper-based optode: Towards a selective cyanide detection, *J. Porphyr. Phthalocyanines* **24**(05n07), 964-972 (2020). https://doi.org/10.1142/S1088424620500091